the FEBS Journal

The mitochondrial protein frataxin is essential for heme biosynthesis in plants

María V. Maliandi[1], Maria V. Busi[2], Valeria R. Turowski[2], Laura Leaden[2], Alejandro Araya[3] and Diego F. Gomez-Casati[2]

1 Instituto de Investigaciones Biotecnológicas-Instituto Tecnológico de Chascomús (IIB-INTECH) CONICET/UNSAM, Argentina
2 Centro de Estudios Fotosintéticos y Bioquímicos (CEFOBI-CONICET), Universidad Nacional de Rosario, Argentina
3 Microbiologie Cellulaire et Moléculaire et Pathogénicité, UMR 5234, Centre National de la Recherche Scientifique and Université Victor Segalen-Bordeaux 2, France

Keywords
Arabidopsis; catalase; frataxin; hemeproteins; mitochondria

Correspondence
D. F. Gomez-Casati, Centro de Estudios Fotosintéticos y Bioquímicos (CEFOBI-CONICET), Universidad Nacional de Rosario, Suipacha 531, 2000, Rosario, Argentina
Fax: +54 341 437 0044
Tel: +54 341 437 1955
E-mail: gomezcasati@cefobi-conicet.gov.ar

(Received 21 July 2010, revised 15 October 2010, accepted 18 November 2010)

doi:10.1111/j.1742-4658.2010.07968.x

Frataxin, a conserved mitochondrial protein implicated in cellular iron homeostasis, has been involved as the iron chaperone that delivers iron for the Fe–S cluster and heme biosynthesis. However, its role in iron metabolism remains unclear, especially in photosynthetic organisms. In previous work, we found that frataxin deficiency in *Arabidopsis* results in decreased activity of the mitochondrial Fe–S proteins aconitase and succinate dehydrogenase, despite the increased expression of the respective genes, indicating an important role for *Arabidopsis thaliana* frataxin homolog (AtFH). In this work, we explore the hypothesis that AtFH can participate in heme formation in plants. For this purpose, we used two *Arabidopsis* lines, *atfh-1* and as-AtFH, with deficiency in the expression of AtFH. Both lines present alteration in several transcripts from the heme biosynthetic route with a decrease in total heme content and a deficiency in catalase activity that was rescued with the addition of exogenous hemin. Our data substantiate the hypothesis that AtFH, apart from its role in protecting bioavailable iron within mitochondria and the biogenesis of Fe–S groups, also plays a role in the biosynthesis of heme groups in plants.

Introduction

Frataxin, a mitochondrial protein encoded by the nuclear genome, plays an essential role in mitochondria biogenesis and is required for cellular iron homeostasis regulation in different organisms [1–3]. Frataxin deficiency in humans causes the cardio- and neurodegenerative disease Friedreich's ataxia, causing progressive mitochondrial iron accumulation, severe disruption of Fe–S cluster biosynthesis and increased oxidative stress [4–8]. This protein is highly conserved from bacteria to mammals and plants without major structural changes, suggesting that frataxin could play an analogous role in all these organisms. The frataxin (*YFH1*) null mutant of *Saccharomyces cerevisae* displays a mitochondrial dysfunction phenotype characterized by a decrease in respiration rate [4,9] and an increase in mitochondrial iron content inducing hypersensitivity to oxidative stress [10]. In addition, it has also been reported that YFH1 binds to the central iron sulfur cluster (ISC) assembly complex, suggesting an important function in early steps of Fe–S protein biogenesis [11]. Thus, it has been postulated that this protein is involved in cellular respiration, iron homeostasis and Fe–S cluster biogenesis [5,12–14].

Previously, we cloned and characterized the *Arabidopsis thaliana* frataxin homolog (AtFH) [15–18]. The functionality of AtFH was assessed by complementation of a yeast frataxin null mutant, suggesting that

Abbreviations
ALA, 5-aminolevulinic acid; AtFH, *Arabidopsis thaliana* frataxin homolog; FC, ferrochelatase.

AtFH was involved in plant mitochondrial respiration and stress responses [16]. Consistent with this hypothesis, AtFH-deficient plants presented a retarded growth, increased production of reactive oxygen species and the induction of oxidative stress markers, characteristic of an oxidative stress state. Interestingly, we also found an induction of aconitase and succinate dehydrogenase subunit (*SDH2-1*) transcripts, coding for two mitochondrial Fe–S-containing proteins. The fact that the activities of both enzymes were reduced in cell extracts indicates that AtFH also participates in Fe–S cluster assembly or their insertion of Fe–S moiety into apoproteins [15]. Consistent with the critical role of AtFH in cell physiology is the observation that homozygous null mutants result in a lethal phenotype [15,19].

Studies in yeast lacking frataxin showed that mitochondrial iron is unavailable for heme synthesis, suggesting that frataxin could have a role as a mitochondrial iron donor involved in heme metabolism [20–22]. Indeed, it has also been reported that human frataxin interacts with ferrochelatase (FC), the enzyme involved in iron assembly to protoporphyrin IX [21,23]. Moreover, Yoon & Cowan [24] demonstrated that frataxin serves as a potential donor to FC for insertion of iron into the protoporphyrin ring during heme synthesis. Knocking down the expression of frataxin in human cells revealed significant defects in the activity of several Fe–S-containing proteins, a reduction of heme a and concomitantly the cytochrome oxidase activity, suggesting an important role of frataxin in the biogenesis of heme-containing proteins [25].

Although the participation of frataxin in delivering iron to heme synthesis is frequently mentioned in the literature, scarce direct evidence exists on the role of this protein in the biogenesis of heme-containing proteins in plants. To gain insight into this process, we decided to study the role of frataxin using the enzyme catalase as a model. Catalase (H_2O_2 oxidoreductase, EC 1.11.1.6) is a hemeprotein involved in the dismutation of H_2O_2 to water and oxygen. Together with superoxide dismutases and hydroperoxidases, catalase is involved in a defense system for the scavenging of superoxide radicals and hydroperoxides [26]. In *Arabidopsis*, three genes named *CAT1*, *CAT2* and *CAT3* encoding different catalase subunits have been described [27]. Here we present evidence that AtFH deficiency results in alteration of mRNAs of heme pathway genes, and a deficiency in heme content and catalase activity.

Results

It has been proposed that frataxin could be involved in the regulation of iron availability within cells [5,28]. As this could have consequences on the biogenesis of cellular Fe–S clusters and the heme groups, we decided to investigate the effect of AtFH deficiency on heme content and the activity of hemeproteins in *Arabidopsis* plants.

Construction of the antisense *as-AtFH* line and phenotypic characterization

The *Arabidopsis* knockdown mutant (*atfh-1*, SALK_021263), deficient in frataxin expression [15], and a frataxin-deficient transgenic antisense line (*as-AtFH*) constructed by transformation with pCAMBIA1302 [29] (Fig. 1A) were used. Transcription analysis of

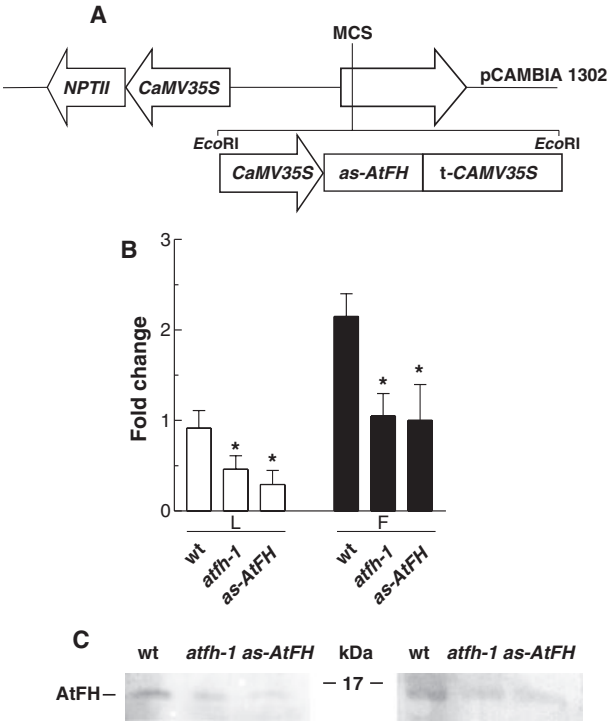

Fig. 1. (A) Scheme of the *as-AtFH* construct used to generate transgenic plants expressing an *AtFH* fragment (564 bp) in antisense orientation. *as-AtFH* is under the control of cauliflower mosaic virus 35S (*CaMV35S*) promoter from pDH51 vector subcloned at the *Eco*RI site from pCAMBIA 1302. MCS, multiple cloning site; t-*CAMV35S*, 35S terminator; *NPTII*, kanamycin resistance gene. (B) qRT-PCR analysis of *AtFH* expression in leaves (L) or flowers (F) from wild-type (wt), *atfh-1* and *as-AtFH* lines. The asterisk signals a statistically different result from the control value ($P < 0.05$). Bars represent mean values (error ± standard deviation) of three independent experiments. Relative AtFH expression levels are shown as fold change values with respect to *β-actin* mRNA levels. (C) Western-blot detection of AtFH protein in wild-type (wt), *atfh-1* and *as-AtFH* lines in leaves (left panel) or flowers (right panel) using serum anti-recombinant AtFH.

mutants by qRT-PCR analysis showed that AtFH mRNA levels were decreased in leaves and flowers of both *atfh-1* and *as-AtFH* lines (Fig. 1B). In addition, AtFH protein levels determined by western blot using specific antibodies showed a decrease of ~50–70% in *atfh-1* and *as-AtFH* lines, respectively (Fig. 1C).

Using the growth conditions described in the experimental section, the *as-AtFH* line showed retarded growth (as also described for the *atfh-1* line [15]) at different developmental stages compared with wild-type plants (Fig. 2). Moreover, as we reported previously for the *atfh-1* line, we did not observe significant differences in the morphology of *as-AtFH* roots, leaves or flowers, but a decrease of ~35% of fruit fresh weight, alteration in silique length and a reduced number of viable seeds (28 ± 6 seeds per silique) compared with 47 ± 5 seeds per silique found in the wild-type (Fig. 2D).

Decrease in heme content in AtFH-deficient plants

The heme content in rosette leaves was reduced to ~34 and 41% in *atfh-1* and *as-AtFH* plants, respectively, whereas in flower tissues the levels fell to 25% in both transgenic lines (Fig. 3). These results indicate that AtFH-deficient plants have altered heme content, agreeing with the proposed hypothesis. Thus, the frataxin-deficient plants constitute a good model to study the biogenesis of cellular hemeproteins.

Alteration of heme pathway transcripts in plants with AtFH deficiency

To better understand the effect of AtFH deficiency on heme biosynthesis, we evaluated the mRNA levels of several transcripts coding for enzymes playing a role in the heme metabolic pathway (see Fig. S1).

First, we investigated the expression levels of *HEMA1* (At1g58290) and *HEMA2* (At1g09940), two genes coding for glutamyl-tRNA reductase proteins that catalyze the production of 5-aminolevulinic acid (ALA). We found that *HEMA1* is downregulated in leaves without significant changes in flowers, whereas *HEMA2* is downregulated in both tissues (Fig. 4A). The levels of *GSA1* (At5g63570) and *GSA2* (At3g48730), two glutamate-1-semialdehyde aminomutase genes involved in the conversion of glutamate-1-semialdehyde into 5-aminolevulinate were also determined. *GSA1* and *GSA2* mRNA levels were reduced ~50% in leaves from AtFH-deficient lines, compared with wild-type plants. By contrast, in flowers, transcript levels of *GSA1* and *GSA2* presented an augment of two- and three-fold compared with the values found in wild-type plants (Fig. 4B).

We also evaluated the transcription levels of two porphobilinogen synthase genes, *HEMB1* (At1g69740) and *HEMB2* (At1g44318). A decrease in *HEMB1* and *HEMB2* transcript levels was found in leaves, whereas no change in *HEMB1* transcript levels was found in flowers (Fig. 4C). By contrast, a three- and eight-fold induction in *HEMB2* mRNA levels was found in flowers of *atfh-1* and *as-AtFH* lines, respectively (Fig. 4C). Furthermore, coproporfirinogen oxidase (*HEMF2*, At4g03205) mRNA levels in leaves showed a 50 and 70% decrease in *atfh-1* and *as-AtFH* lines, compared with wild-type, whereas no significant changes in their amount were observed in flowers of these lines (Fig. 4D).

Finally, we analyzed the expression of two FC genes, *AtFC-1* (At5g26030) and *AtFC-2* (At2g30390). *AtFC-1* has been found to be expressed in all plant

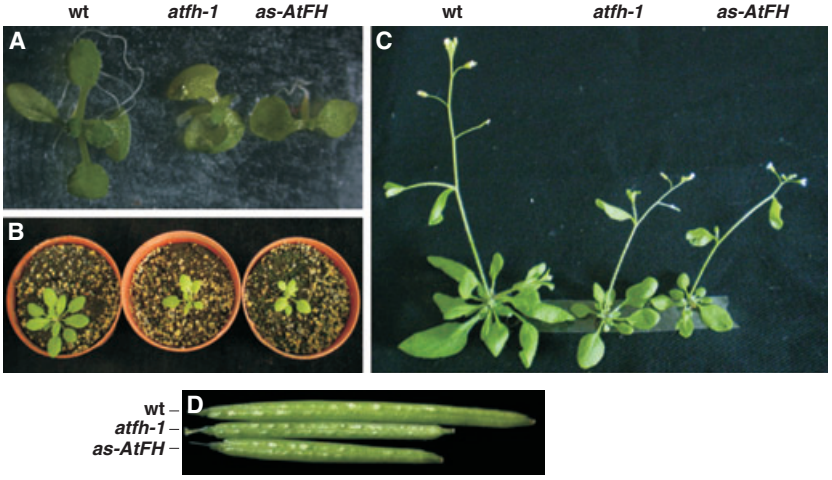

Fig. 2. Phenotype comparison of wild-type (wt), *atfh-1* and *as-AtFH* plants at different stages of development: 14-day-old (A); 21-day-old (B) and 40-day-old (C) growth plants. (D) Morphology of siliques (8–10 days post anthesis) from wild-type (wt), *atfh-1* and *as-AtFH* lines.

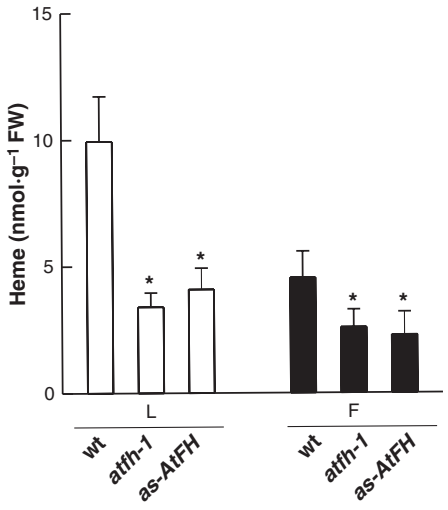

Fig. 3. Noncovalently bound heme quantification in leaves (L, white bars) or flowers (F, black bars) from wild-type (wt), *atfh-1* and *as-AtFH* lines. The asterisk signals a statistically different result from the control value ($P < 0.05$). Values are the mean ± standard deviation of four independent replicates.

tissues and mainly in flowers and roots with an enhanced expression under oxidative stress conditions or tissue damage [30]. *AtFC-2* is expressed in all plant tissues, except in roots. An induction of ~1.5–2-fold in *AtFC-1* levels was found in AtFH-deficient leaves by QPCR analysis (Fig. 4E). By contrast, no significant changes in *AtFC-1* mRNA and a slight decrease in *AtFC-2* mRNA levels were detected in flowers (Fig. 4E). In agreement with these results, AtFC activity in leaves showed an increase of ~15% in AtFH-deficient plants, whereas no significant changes were observed in flowers (not shown). These data suggest that AtFH deficiency has a minor effect on AtFC activity.

AtFH deficiency affects catalase activity but not their mRNA or protein levels

To assess the impact of AtFH deficiency on the activity of heme-containing proteins, we decided to investigate the catalase enzymes that catalyze the dismutation of H_2O_2 to H_2O and O_2. In plants, H_2O_2 is removed essentially by three enzymes: catalase, ascorbate peroxidase and glutathione peroxidase [31]. Catalases do not consume reducing power and have a very high reaction rate, whereas ascorbate peroxidase and glutathione peroxidase require a source of reductant, ascorbate or glutathione. Therefore, although plants contain different H_2O_2 metabolizing enzymes, catalases are highly active enzymes in the absence of reductants as they primarily catalyze a dismutase reaction [32]. H_2O_2 consumption was measured in the absence of other reductants and using a protocol previously reported for the determination of catalase activity in plants (see Materials and Methods section). Under this condition, the activity detected can be attributed mainly to catalases.

Total catalase activity was determined in leaves and flowers from AtFH-deficient lines. In both lines, a decrease of ~20% in catalase activity was found in leaves (Fig. 5A), whereas a reduced activity of 15 and 40% was observed in flowers from *atfh-1* and *as-AtFH* lines, respectively.

In *Arabidopsis*, three genes coding for catalase, *CAT1* (At1g20630), *CAT2* (At4g35090) and *CAT3* (At1g20620), have been described. CAT2, located in peroxisomes/glyoxisomes and cytosol, is the major isoform in leaves, whereas CAT1 (located mainly in cytosol and peroxisomes) and CAT3 (located in mitochondria) are less abundant [27]. Interestingly, the mRNA levels of the genes encoding the three catalase isoforms show no significant differences when compared with wild-type plants (Fig. 5B). Western blot analysis of leaf and flower extracts revealed with anti-catalase IgG showed no significant differences between AtFH-deficient and wild-type plants (Fig. 5C). These results indicate that AtFH deficiency does not affect catalase expression, but has an impact on the catalytic activity in leaves and flowers.

Hemin rescues catalase activity in cell suspension cultures and isolated mitochondria

To examine if the decrease in catalase activity results from a heme deficiency, we determined the enzymatic activity in *atfh-1* and *as-AtFH* cell suspension cultures using different concentrations of ALA, protoporphyrin IX and hemin. It has been reported that hemin itself has a catalase-like activity [33]. Therefore, we carried out the assay of catalase activity in wild-type cells without additions or in the presence of 1–10 μM hemin. Under the conditions described above, the activity of hemin does not have a significant contribution to the total catalase activity (Fig. 6A). In agreement with the data shown in Fig. 5A, we also observed a decrease in catalase activity in *Arabidopsis* cells. On the other hand, an almost complete restoration of catalase activity was observed in both AtFH-deficient lines after incubation with 5 and 10 μM hemin (Fig. 6A), whereas no changes were found in the presence of protoporphyrin IX or ALA (Fig. 6B, C). It should be noted that no significant differences in *AtFH* mRNA levels were detected after incubation with hemin, protoporphyrin IX or ALA (not shown).

The effect of hemin, protoporphyrin IX and ALA treatment on catalase activity in isolated mitochondria

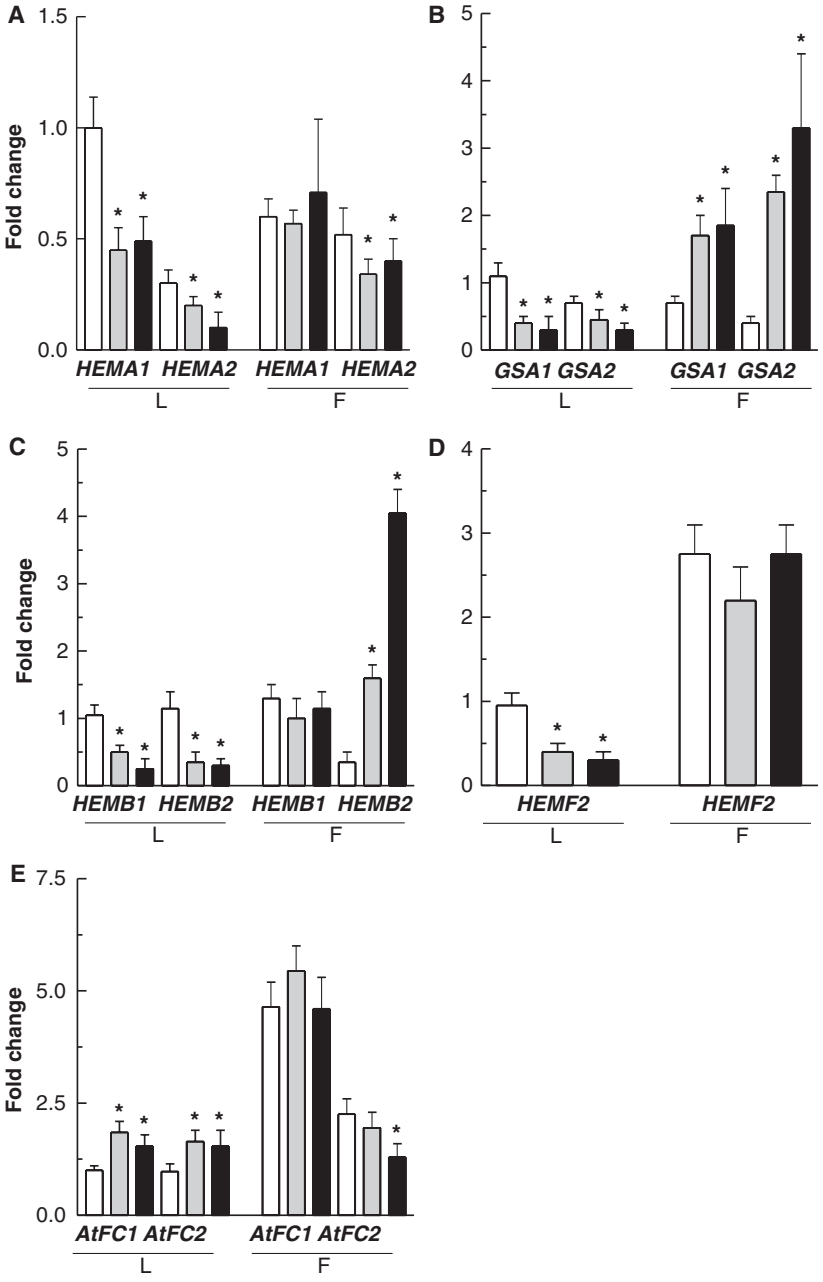

Fig. 4. qRT-PCR analysis of genes involved in the heme biosynthetic pathway: (A) glutamyl tRNA reductase (*HEMA1*, At1g58290 and *HEMA2*, At1g09940); (B) glutamate-1-semialdehyde aminomutase (*GSA1*, At5g63570 and *GSA2*, At3g48730); (C) porphobilinogen synthase (*HEMB1*, At1g69740 and *HEMB2*, At1g44318); (D) coproporphyrinogen oxidase (*HEMF2*, At4g03205); (E) FC (*AtFC-1*, At5g26030 and *AtFC-2*, At2g30390). RNA was extracted from rosette leaves (L) or flowers (F, stage 12) from wild-type (white bars), *atfh-1* (grey bars) and *as-AtFH* (black bars) plants. The asterisk signals a statistically different result from the control value ($P < 0.05$). Columns represent mean values (error bars ± standard deviation) of three independent experiments. Relative expression levels are shown as fold change values with respect to *β-actin* mRNA levels.

from *atfh-1* and *as-AtFH* plants was studied. A decrease of 40 and 51% of catalase activity was found in AtFH-deficient mitochondria. The activity was almost completely restored after incubation of the organelle suspension with 10 μM hemin (Fig. 6D). By contrast, no significant changes in catalase activity were observed in the presence of protoporphyrin IX or ALA in *atfh-1* and *as-AtFH* lines.

In addition, the catalase activity was not affected when isolated mitochondria were incubated with protoporphyrin IX in the presence of 1 or 5 μM Fe(II) in citrate-buffered solutions (see Fig. S2). Moreover, the levels of FC activity measured in isolated mitochondria extracts were close to the background value (not shown). These results agree with those previously reported on the possibility that ferrous ions can be inserted nonenzymatically into phorphyrin in the presence of reductants or fatty acids, but this reaction does not occur *in vivo* [34].

Discussion

The understanding of the role of frataxin in iron homeostasis in plants becomes highly relevant because

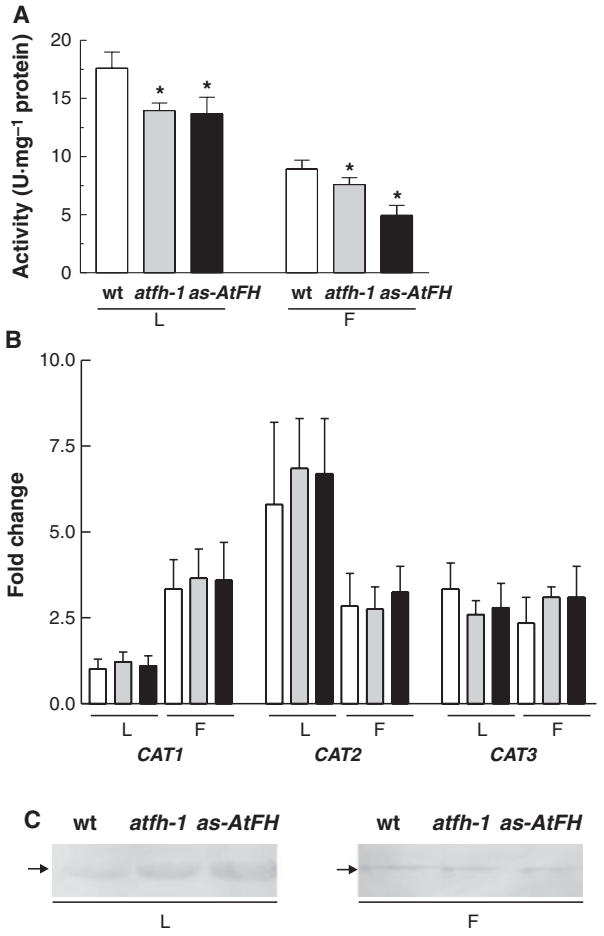

Fig. 5. (A) Enzymatic activity of catalase from wild-type (wt), *atfh-1* and *as-AtFH* lines analyzed in rosette leaves (L) or flower extracts (F, stage 12). (B) qRT-PCR analysis of catalase genes in leaves (L) and flowers (F) from wild-type, *atfh-1* and *as-AtFH* lines (*CAT1*, At1g20630; *CAT2*, At4g35090 and *CAT3*, At1g20620): wild-type (white bars), *atfh-1* (grey bars), *as-AtFH* (black bars). Columns represent mean values (error bars ± standard deviation) of three independent experiments. Relative expression levels are shown as fold change values with respect to *β-actin* mRNA levels. (C) Western blot analysis of catalase protein from leaves (L) or flower (F) extracts from wild-type (wt), *atfh-1* and *as-AtFH* lines using specific anti-catalase IgG.

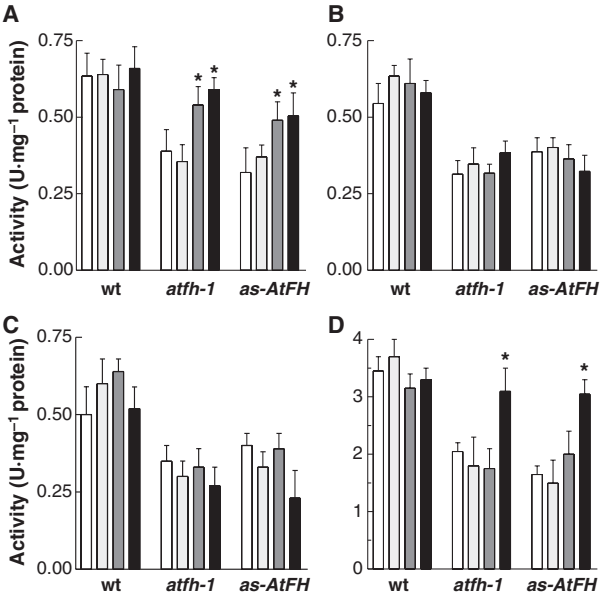

Fig. 6. (A) Determination of total catalase activity in homogenates obtained from cell culture extracts from wild-type (wt), *atfh-1* and *as-AtFH* lines in the absence (white bars) or in the presence of different concentrations of hemin: 0.5 μM (light grey bars); 5 μM (dark grey bars) or 10 μM (black bars). (B, C) Determination of catalase activity in homogenates obtained from cell culture extracts from wild-type (wt), *atfh-1* and *as-AtFH* lines in the absence (white bars) or in the presence of different concentrations of protoporphyrin IX (B) or ALA (C): 0.5 μM (light grey bars); 5 μM (dark grey bars) or 10 μM (black bars). (D) Total catalase activity determined in mitochondrial suspensions from wild-type (wt), *atfh-1* and *as-AtFH* lines without additions (white bars) or in the presence of 10 μM protoporphyrin IX (light grey bars), ALA (dark grey bars) or 10 μM hemin (black bars). The asterisk indicates values statistically different from the control ($P < 0.05$). Columns represent mean values (error bars ± standard deviation) of three independent experiments.

of its association with Fe–S clusters and heme groups, the two main iron-containing prosthetic groups that participate in the catalysis of numerous biochemical reactions. However, the connection between both pathways, as well as the role of frataxin in iron metabolism, remain unclear, especially in photosynthetic organisms. Iron as a cofactor is involved in many cellular processes: (a) biogenesis of Fe–S proteins accomplished by the Fe–S cluster machinery located in the mitochondrial matrix [35] and (b) biogenesis of heme groups and hemeproteins. The respiratory complexes of the mitochondrial inner membrane involved in energetic metabolism, aconitase and many other proteins with different subcellular locations require Fe–S clusters for activity [2,36]. On the other hand, cytochromes and catalases require the presence of heme as a cofactor for function [37,38].

Yeast cells lacking frataxin, YFH, are deficient in iron use by FC and show low cytochrome content, suggesting that the iron used in heme synthesis is under the control of YFH [21]. Furthermore, yeast mutants with deficiencies in the mitochondrial Fe–S cluster assembly machinery display reduced levels of heme-containing proteins such as cytochromes and cytochrome *c* oxidase, suggesting a deficiency in the heme pathway [39]. In addition, Zhang *et al.* [40,41] reported that YFH and two mitochondrial carrier proteins, MRS3 and MRS4 implicated in iron homeostasis, have a cooperative

function in providing iron for heme and Fe–S synthesis in yeasts. Thus, it was proposed that frataxin could have a role in the modulation of iron availability within mitochondria for Fe–S and heme group synthesis and frataxin deficiency might have an impact in Fe–S and heme-containing protein biogenesis.

On the other hand, it has been reported that frataxin interacts with FC and mediates iron delivery in the final step of heme synthesis in human mitochondria [24]. However, there is no strong evidence for the presence of FC in plant mitochondria. Cornah *et al.* [30] and Masuda *et al.* [42] reported that most FC activity was associated with plastids. Lister *et al.* [43] found that either of the two FC isoforms from *A. thaliana* were imported into chloroplasts *in vitro*. Masuda *et al.* [42] found that GFP-fusion proteins with either of two isoforms of FC from cucumber were targeted to plastids, but not to mitochondria. Indeed, the specific antibodies against either of the two isoforms of FC detected signals only in plastids [42]. In *Chlamydomonas reinhardtii*, where a single gene encodes for FC, the protein is targeted into the plastids, indicating that the FC activity is not required to be present inside mitochondria [44]. Thus, it has been suggested that in plants the synthesis of heme takes place almost exclusively in plastids and exported to cytosol and mitochondria [44–46]. Consistent with these results, we found less than 0.3% FC total activity in isolated mitochondria, corroborating the data reported by Cornah *et al.* [30].

It has been suggested that frataxin deficiency causes defects late in the heme pathway. The transcriptome analysis of human lymphoblasts derived from Friedreich's ataxia patients and frataxin-deficient mice showed a decrease in the mRNA levels of coproporphyrinogen oxidase and delta-aminolevulinate synthase 1, two enzymes involved in the heme biosynthetic pathway, and also Isu1 and FC. These observations support the idea that frataxin deficiency affects the expression of many nuclear-encoded mitochondrial genes [47]. This situation is associated with increased levels of protoporphyrin IX, consistent with a defect downstream of this metabolite in the heme pathway [47]. In addition, reduced mitochondrial heme a and heme c levels and a decreased activity of cytochrome oxidase strongly suggest that frataxin is involved in late stages of the heme biosynthetic pathway, i.e., the incorporation of iron into protoporphyrin IX to produce heme [21,47,48]. It has been reported that the key control point of heme and chlorophyll synthesis in plants is the formation of ALA from glutamate catalyzed by glutamyl-tRNA reductase enzymes encoded by *HEMA* genes [49]. *HEMA1* has been associated with the provision of tetrapyrroles for chlorophyll and heme production in photosynthetic tissues, whereas the role of *HEMA2* is to provide a background activity of glutamyl-tRNA reductase for heme production, mainly in nonphotosynthetic tissues [50,51]. Thus, the downregulation of both *HEMA1* and *HEMA2* transcripts is in agreement with the observed heme deficiency in AtFH-deficient plants.

Arabidopsis AtFH-deficient lines also showed a modification of the mRNA levels of other enzymes involved in heme biosynthesis, such as GSA1 and 2, HEMB1, and 2, HEMF2 and FC1 and FC2, indicating that an analogous situation occurs in plants. However, a different response was found when compared in different organs. In flowers, *GSA1* and *GSA2* transcript levels were increased compared with leaves, where the respective transcripts were downregulated or remain unchanged. It should be noted that a differential response for some isoforms was observed in flowers but not in leaves. The *HEMB2* transcript level was increased several fold, whereas *HEMB1* mRNA levels remained unchanged in flowers. Also, a decrease in mRNA levels for *AtFC2* contrast with the unmodified expression pattern of *AtFC1*. The different expression pattern of these genes in leaves and flowers could be explained by a differential regulation, probably reflecting the gene expression network specific to each organ. These observations should be interpreted with caution, as it is difficult to know whether the observed effect is directly linked to AtFH deficiency or is the result of a secondary event. Previously, we found that AtFH-deficient plants present increased reactive oxygen species formation [15,16]. The reactive oxygen species have been implicated in complex gene expression responses, particularly the induction of nuclear-encoded mitochondrial genes [52].

Catalase activity was reduced in AtFH-deficient plants without significant reduction of catalase mRNAs or protein levels. The fact that the decrease in catalase activity correlates with the deficiency in heme content, and the observation that the normal enzymatic activity is recovered after addition of hemin, but not the iron-lacking tetrapyrrole protoporphyrin IX or ALA, substantiate the hypothesis that AtFH would have a major role in heme production required for the formation of the active catalase holoenzyme. This effect is particularly evident for the catalase activity associated with the mitochondria fraction where CAT3 is the main isoform. These results are in accordance with hemin rescue experiments performed in frataxin-deficient neuronal cells, which showed increased activity of some Fe–S protein and cytochrome oxidase restoring the normal phenotype [25], and with data showing that recombinant erythropoietin, which

stimulates the synthesis of heme, can rescue the phenotype observed in frataxin-deficient cells [53].

In summary, AtFH-deficient plants present alteration in several transcripts from the heme biosynthetic route with a decrease in total heme content and a deficiency of catalase activity that can be rescued by exogenous hemin, indicating that AtFH, apart from its role in protecting bioavailable iron within mitochondria and the synthesis of Fe–S groups, also plays a role in the production of heme groups and the activity of hemeproteins in plants.

Materials and Methods

Plant material and growth conditions

Arabidopsis thaliana (var. Columbia Col-0) was used as the wild-type reference plant. Two frataxin-deficient lines were also used in these experiments: a T-DNA knockdown mutant (*atfh-1*, SALK_021263) and an antisense line, *as-atfh*. Mutant plants were selected in MS agar medium containing 30 $g \cdot mL^{-1}$ kanamycin. Transgenic *as-AtFH* plants were selected in MS medium containing 20 $\mu g \cdot mL^{-1}$ hygromycin. After 2 weeks, plants were transferred to soil and grown in a greenhouse, at 25 °C under fluorescent lamps (Grolux, Sylvania, Danvers, MA, USA and Cool White, Philips, Amsterdam, The Netherlands) with an intensity of 150 $\mu mol \cdot m^{-2} \cdot s^{-1}$ using a 16 h light/8 h dark photoperiod. *Arabidopsis* cell suspension cultures were grown in the dark (22 °C) in an orbital shaker (130 r.p.m.).

Isolation of RNA and qRT-PCR analysis

Total RNA was extracted from rosette leaves and flowers (stage 12) using the RNA plant mini kit (Qiagen, Valencia, CA, USA). Complementary DNA was synthesized using random hexamers and the M-MLV reverse transcriptase protocol (USB Corp., Cleveland, OH, USA). qRT-PCR was carried out in a MiniOPTICON2 apparatus (BioRad, Hercules, CA, USA), using the intercalation dye SYBR-Green I (Invitrogen, Carlsbad, CA, USA) as a fluorescent reporter and Go Taq polymerase (Promega, Madison, WI, USA). Primers suitable for amplification of 150–250 bp products for each gene under study were designed using the PRIMER3 software (see Table S1). Amplification of cDNA was carried out under the following conditions: 2 min denaturation at 94 °C; 40–45 cycles at 94 °C for 15 s, 57 °C for 20 s, and 72 °C for 20 s, followed by 10 min extension at 72 °C. Three replicates were performed for each sample. Melting curves for each PCR were determined by measuring the decrease in fluorescence with increasing temperature (from 65 to 98 °C). PCR products were run on a 2% (w/v) agarose gel to confirm the size of the amplification products and to verify the presence of a unique PCR product. Relative transcript levels were calculated as a ratio of the transcript abundance of the studied gene to the transcript abundance of *β-actin* (At3g18780).

Production of *as-atfh* transgenic plants

To prepare the antisense construct of frataxin, a *Bam*HI/*Sma*I fragment containing the *AtFH* coding sequence (564 bp) was obtained by PCR (see primers used in Table S1) and then cloned downstream from the cauliflower mosaic virus 35S promoter into the pDH51 vector [54] previously digested with *Bam*HI and *Sma*I. After verifying the correct orientation of the insert, the resulting *35S:as-AtFH* expression cassette was excised as *Eco*RI restriction fragments and subcloned into pCAMBIA 1320 [29]. The recombinant plasmids were introduced into *Agrobacterium tumefaciens* GV3101 strain by the freeze–thaw method [55]. *Arabidopsis* was transformed using the floral dip method [56]. The expression of the antisense version of *AtFH* was verified by RT-PCR.

Determination of heme content

The content of noncovalently bound heme was determined using 6 week rosette leaves or flowers (stage 12) from wild-type, *atfh-1* and *as-AtFH*, as previously described [57]. Extracted heme was spectrophotometrically quantified with a Perkin–Elmer lambda 35 UV/Vis spectrometer by measuring the absorbance at 398 nm (Perkin–Elmer, Boston, MA, USA). Standard solutions of hemin (Sigma-Aldrich, St Louis, MO, USA) were prepared by dissolving the solid reagent in 50 mM sodium phosphate buffer, pH 7.4.

Enzyme assays

Homogenates from cell cultures were prepared as follows: 1–2 g of cells were centrifuged for 10 min at 3000***g*** and the pellet was ground to a powder with liquid nitrogen. The powdered material was homogenized with extraction buffer containing 450 mM sucrose, 15 mM Mops-KOH, 1.5 mM EGTA and 6 $g \cdot L^{-1}$ polyvinylpyrrolidone, pH 7.4. The suspension was incubated with 2 $g \cdot L^{-1}$ BSA, 0.2 mM phenylmethanesulfonyl fluoride and 500 U cellulase (ICN Biomedicals, Aurora, OH, USA) at 4 °C for 60 min. Cells were disrupted using an ultrasonicator (VCX130, Sonics & Materials, Newtown, CT, USA) and centrifuged at 10 000***g*** for 20 min at 4 °C and the supernatant collected. The homogenate from *Arabidopsis* tissues (leaves and flowers) was prepared as follows: ~200 mg tissue was frozen under liquid nitrogen and ground to a powder. The powdered material was homogenized in extraction buffer (50 mM KH_2PO_4 pH 7.8, 0.5% v/v Triton X-100, 0.5 mM EDTA and 1 mM phenylmethanesulfonyl fluoride). The homogenate was centrifuged at 9500 ***g*** for 20 min at 4 °C and the supernatant collected. Catalase activity was determined at

25 °C as described previously [58] with minor modifications [59] by following the decrease in absorbance (A) at 240 nm at 25 °C. The catalase assay medium contained 470 μL of 50 mM KH_2PO_4 pH 7.0 and 10 mM H_2O_2 as a substrate. Homogenates used to determine FC activity were prepared as previously described [60] and enzymatic activity was measured according to previous methods [61].

Porphyrin and ALA treatments

Hemin, protoporphyrin IX or ALA (0–10 μM) were added to 100 mL of *Arabidopsis* cell cultures and incubated at 24 °C for 18 h with orbital shaking. Catalase activity was determined as described in the previous section. Mitochondria suspensions (~10 $mg \cdot mL^{-1}$ protein) were incubated in a buffer containing 250 mM mannitol, 50 mM KCl, 2 mM $MgCl_2$, 20 mM Hepes pH 7.4, 1 mM K_2HPO_4, 1 mM dithiothreitol, 10 mM ATP, 20 μM ADP, 10 mM sodium succinate and 10 μM hemin, protoporphyrin IX or ALA for 2 h with constant shaking. After incubation, mitochondria were recovered by centrifugation and resuspended in 10 mM KH_2PO_4 pH 7. After lysis using an ultrasonicator (VCX130, Sonics & Materials) followed by centrifugation at 12 000***g*** for 10 min, the catalase activity was determined in the supernatant using the assay described above.

Additional methods

Isolation of highly purified mitochondria from *Arabidopis* leaves and flowers was carried out as described by Werhahn *et al.* [62,63] with modifications. Under these conditions, the mitochondrial fraction is essentially deprived of cytoplasmic and plastid contamination. The mitochondrial pellet was recovered with buffer containing 300 mM mannitol and 10 mM K_2HPO_4 (pH 7.4) as previously described [15]. Proteins were separated by electrophoresis on 12% SDS/PAGE [64] and revealed by Coomassie Blue staining or electroblotted on to nitrocellulose membranes (BioRad). Electroblotted membranes were incubated with anti-recombinant AtFH or anti-catalase (kindly provided by M. Nishimura, National Institute for Basic Biology, Okazaki, Japan) polyclonal IgG. The antigen–antibody complex was visualized with alkaline phosphatase-linked anti-mouse IgG or anti-rabbit IgG, followed by staining with 5-bromo-4-chloroindol-2-yl phosphate and Nitro Blue tetrazolium as described previously [65]. Total protein was determined as described by Bradford [66]. The relative protein levels in western blots were determined by densitometric analysis using the GEL PRO ANALYZER program (Media Cybernetics, Bethesda, MD, USA).

Statistical analyses

The significance of differences was determined using Student's *t*-test. Values statistically different from the control ($P < 0.05$) are denoted with an asterisk in Figs 1, 3–6.

Acknowledgements

This work was supported by grants from PICS-CNRS 3641, the Université Victor Segalen Bordeaux 2, ANPCyT (PICT 00614 and 0729). MVM and VRT are doctoral fellows from CONICET. LL is a doctoral fellow from ANPCyT. MVB and DGC are research members from CONICET.

References

1 Bencze KZ, Kondapalli KC, Cook JD, McMahon S, Millan-Pacheco C, Pastor N & Stemmler TL (2006) The structure and function of frataxin. *Crit Rev Biochem Mol Biol* **41**, 269–291.
2 Lill R & Mühlenhoff U (2008) Maturation of iron-sulfur proteins in eukaryotes: mechanisms, connected processes, and diseases. *Annu Rev Biochem* **77**, 669–700.
3 Lill R (2009) Function and biogenesis of iron-sulphur proteins. *Nature* **460**, 831–838.
4 Campuzano V, Montermini L, Molto MD, Pianese L, Cossee M, Cavalcanti F, Monros E, Rodius F, Duclos F, Monticelli A *et al.* (1996) Friedreich's ataxia: autosomal recessive disease caused by an intronic GAA triplet repeat expansion. *Science* **271**, 1423–1427.
5 Babcock M, de Silva D, Oaks R, Davis-Kaplan S, Jiralerspong S, Montermini L, Pandolfo M & Kaplan J (1997) Regulation of mitochondrial iron accumulation by Yfh1p, a putative homolog of frataxin. *Science* **276**, 1709–1712.
6 Pandolfo M (2002) Frataxin deficiency and mitochondrial dysfunction. *Mitochondrion* **2**, 87–93.
7 Puccio H (2009) Multicellular models of Friedreich ataxia. *J Neurol* **256**(Suppl 1), 18–24.
8 Schmucker S & Puccio H (2010) Understanding the molecular mechanisms of Friedreich's ataxia to develop therapeutic approaches. *Hum Mol Genet* **19**, R103–110.
9 Koutnikova H, Campuzano V, Foury F, Dolle P, Cazzalini O & Koenig M (1997) Studies of human, mouse and yeast homologues indicate a mitochondrial function for frataxin. *Nat Genet* **16**, 345–351.
10 Rotig A, de Lonlay P, Chretien D, Foury F, Koenig M, Sidi D, Munnich A & Rustin P (1997) Aconitase and mitochondrial iron-sulphur protein deficiency in Friedreich ataxia. *Nat Genet* **17**, 215–217.
11 Gerber J, Muhlenhoff U & Lill R (2003) An interaction between frataxin and Isu1/Nfs1 that is crucial for Fe/S cluster synthesis on Isu1. *EMBO Rep* **4**, 906–911.
12 Chen OS, Hemenway S & Kaplan J (2002) Inhibition of Fe-S cluster biosynthesis decreases mitochondrial iron export: evidence that Yfh1p affects Fe-S cluster synthesis. *Proc Natl Acad Sci USA* **99**, 12321–12326.

13 Huynen MA, Snel B, Bork P & Gibson TJ (2001) The phylogenetic distribution of frataxin indicates a role in iron-sulfur cluster protein assembly. *Hum Mol Genet* **10**, 2463–2468.
14 Ristow M, Pfister MF, Yee AJ, Schubert M, Michael L, Zhang CY, Ueki K, Michael MD II, Lowell BB & Kahn CR (2000) Frataxin activates mitochondrial energy conversion and oxidative phosphorylation. *Proc Natl Acad Sci USA* **97**, 12239–12243.
15 Busi MV, Maliandi MV, Valdez H, Clemente M, Zabaleta EJ, Araya A & Gomez-Casati DF (2006) Deficiency of *Arabidopsis thaliana* frataxin alters activity of mitochondrial Fe-S proteins and induces oxidative stress. *Plant J* **48**, 873–882.
16 Busi MV, Zabaleta EJ, Araya A & Gomez-Casati DF (2004) Functional and molecular characterization of the frataxin homolog from *Arabidopsis thaliana*. *FEBS Lett* **576**, 141–144.
17 Maliandi MV, Busi MV, Clemente M, Zabaleta EJ, Araya A & Gomez-Casati DF (2007) Expression and one-step purification of recombinant *Arabidopsis thaliana* frataxin homolog (AtFH). *Protein Expr Purif* **51**, 157–161.
18 Martin M, Colman MJ, Gomez-Casati DF, Lamattina L & Zabaleta EJ (2009) Nitric oxide accumulation is required to protect against iron-mediated oxidative stress in frataxin-deficient *Arabidopsis* plants. *FEBS Lett* **583**, 542–548.
19 Vazzola V, Losa A, Soave C & Murgia I (2007) Knockout of frataxin gene causes embryo lethality in *Arabidopsis*. *FEBS Lett* **581**, 667–672.
20 Becker EM, Greer JM, Ponka P & Richardson DR (2002) Erythroid differentiation and protoporphyrin IX down-regulate frataxin expression in Friend cells: characterization of frataxin expression compared to molecules involved in iron metabolism and hemoglobinization. *Blood* **99**, 3813–3822.
21 Lesuisse E, Santos R, Matzanke BF, Knight SAB, Camadro JM & Dancis A (2003) Iron use for haeme synthesis is under control of the yeast frataxin homologue (Yfh1). *Human Mol Genet* **12**, 879–889.
22 Park S, Gakh O, O'Neill HA, Mangravita A, Nichol H, Ferreira GC & Isaya G (2003) Yeast frataxin sequentially chaperones and stores iron by coupling protein assembly with iron oxidation. *J Biol Chem* **278**, 31340–31351.
23 He Y, Alam SL, Proteasa SV, Zhang Y, Lesuisse E, Dancis A & Stemmler TL (2004) Yeast frataxin solution structure, iron binding, and ferrochelatase interaction. *Biochemistry* **43**, 16254–16262.
24 Yoon T & Cowan JA (2004) Frataxin-mediated iron delivery to ferrochelatase in the final step of heme biosynthesis. *J Biol Chem* **279**, 25943–25946.
25 Napoli E, Morin D, Bernhardt R, Buckpitt A & Cortopassi G (2007) Hemin rescues adrenodoxin, heme a and cytochrome oxidase activity in frataxin-deficient oligodendroglioma cells. *Biochim Biophys Acta* **1772**, 773–780.
26 Beyer W, Imlay J & Fridovich I (1991) Superoxide dismutases. *Prog Nucleic Acid Res Mol Biol* **40**, 221–253.
27 Frugoli JA, Zhong HH, Nuccio ML, McCourt P, McPeek MA, Thomas TL & McClung CR (1996) Catalase is encoded by a multigene family in *Arabidopsis thaliana* (L.) Heynh. *Plant Physiol* **112**, 327–336.
28 Radisky DC, Babcock MC & Kaplan J (1999) The yeast frataxin homologue mediates mitochondrial iron efflux. Evidence for a mitochondrial iron cycle. *J Biol Chem* **274**, 4497–4499.
29 Hajdukiewicz P, Svab Z & Maliga P (1994) The small, versatile pPZP family of *Agrobacterium* binary vectors for plant transformation. *Plant Mol Biol* **25**, 989–994.
30 Cornah JE, Roper JM, Pal Singh D & Smith AG (2002) Measurement of ferrochelatase activity using a novel assay suggests that plastids are the major site of haem biosynthesis in both photosynthetic and non-photosynthetic cells of pea (*Pisum sativum* L.). *Biochem J* **362**, 423–432.
31 Rizhsky L, Hallak-Herr E, Van Breusegem F, Rachmilevitch S, Barr JE, Rodermel S, Inze D & Mittler R (2002) Double antisense plants lacking ascorbate peroxidase and catalase are less sensitive to oxidative stress than single antisense plants lacking ascorbate peroxidase or catalase. *Plant J* **32**, 329–342.
32 Willekens H, Chamnongpol S, Davey M, Schraudner M, Langebartels C, Van Montagu M, Inze D & Van Camp W (1997) Catalase is a sink for H2O2 and is indispensable for stress defence in C3 plants. *EMBO J* **16**, 4806–4816.
33 Grinberg LN, O'Brien PJ & Hrkal Z (1999) The effects of heme-binding proteins on the peroxidative and catalatic activities of hemin. *Free Radic Biol Med* **27**, 214–219.
34 Taketani S & Tokunaga R (1984) Non-enzymatic heme formation in the presence of fatty acids and thiol reductants. *Biochim Biophys Acta* **798**, 226–230.
35 Lill R & Kispal G (2000) Maturation of cellular Fe-S proteins: an essential function of mitochondria. *Trends Biochem Sci* **25**, 352–356.
36 Balk J & Lobreaux S (2005) Biogenesis of iron-sulfur proteins in plants. *Trends Plant Sci* **10**, 324–331.
37 Giege P, Grienenberger JM & Bonnard G (2008) Cytochrome c biogenesis in mitochondria. *Mitochondrion* **8**, 61–73.
38 Welinder KG (1992) Superfamily of plant, fungal and bacterial peroxidases. *Curr Opin Struct Biol* **2**, 388–393.
39 Lange H, Muhlenhoff U, Denzel M, Kispal G & Lill R (2004) The heme synthesis defect of mutants impaired

in mitochondrial iron-sulfur protein biogenesis is caused by reversible inhibition of ferrochelatase. *J Biol Chem* **279**, 29101–29108.
40 Zhang Y, Lyver EK, Knight SAB, Lesuisse E & Dancis A (2005) Frataxin and mitochondrial carrier proteins, Mrs3p and Mrs4p, cooperate in providing iron for heme synthesis. *J Biol Chem* **280**, 19794–19807.
41 Zhang Y, Lyver ER, Knight SAB, Pain D, Lesuisse E & Dancis A (2006) Mrs3p, Mrs4p, and frataxin provide iron for Fe–S cluster synthesis in mitochondria. *J Biol Chem* **281**, 22493–22502.
42 Masuda T, Suzuki T, Shimada H, Ohta H & Takamiya K (2003) Subcellular localization of two types of ferrochelatase in cucumber. *Planta* **217**, 602–609.
43 Lister R, Chew O, Rudhe C, Lee MN & Whelan J (2001) *Arabidopsis thaliana* ferrochelatase-I and -II are not imported into *Arabidopsis* mitochondria. *FEBS Lett* **506**, 291–295.
44 van Lis R, Atteia A, Nogaj LA & Beale SI (2005) Subcellular localization and light-regulated expression of protoporphyrinogen IX oxidase and ferrochelatase in *Chlamydomonas reinhardtii*. *Plant Physiol* **139**, 1946–1958.
45 Mochizuki N, Tanaka R, Grimm B, Masuda T, Moulin M, Smith AG, Tanaka A & Terry MJ (2008) The cell biology of tetrapyrroles: a life and death struggle. *Trends Plant Sci* **15**, 488–498.
46 Tanaka R & Tanaka A (2007) Tetrapyrrole biosynthesis in higher plants. *Annu Rev Plant Biol* **58**, 321–346.
47 Schoenfeld RA, Napoli E, Wong A, Zhan S, Reutenauer L, Morin D, Buckpitt AR, Taroni F, Lonnerdal B, Ristow M *et al*. (2005) Frataxin deficiency alters heme pathway transcripts and decreases mitochondrial heme metabolites in mammalian cells. *Human Mol Genet* **14**, 3787–3799.
48 Puccio H, Simon D, Cossee M, Criqui-Filipe P, Tiziano F, Melki J, Hindelang C, Matyas R, Rustin P & Koenig M (2001) Mouse models for Friedreich ataxia exhibit cardiomyopathy, sensory nerve defect and Fe-S enzyme deficiency followed by intramitochondrial iron deposits. *Nat Genet* **27**, 181–186.
49 Papenbrock J & Grimm B (2001) Regulatory network of tetrapyrrole biosynthesis—studies of intracellular signalling involved in metabolic and developmental control of plastids. *Planta* **213**, 667–681.
50 Nagai S, Koide M, Takahashi S, Kikuta A, Aono M, Sasaki-Sekimoto Y, Ohta H, Takamiya K & Masuda T (2007) Induction of isoforms of tetrapyrrole biosynthetic enzymes, AtHEMA2 and AtFC1, under stress conditions and their physiological functions in *Arabidopsis*. *Plant Physiol* **144**, 1039–1051.
51 Ujwal ML, McCormac AC, Goulding A, Kumar AM, Soll D & Terry MJ (2002) Divergent regulation of the HEMA gene family encoding glutamyl-tRNA reductase in *Arabidopsis thaliana*: expression of HEMA2 is regulated by sugars, but is independent of light and plastid signalling. *Plant Mol Biol* **50**, 83–91.
52 Rhoads DM, Umbach AL, Subbaiah CC & Siedow JN (2006) Mitochondrial reactive oxygen species. Contribution to oxidative stress and interorganellar signaling. *Plant Physiol* **141**, 357–366.
53 Sturm B, Stupphann D, Kaun C, Boesch S, Schranzhofer M, Wojta J, Goldenberg H & Scheiber-Mojdehkar B (2005) Recombinant human erythropoietin: effects on frataxin expression in vitro. *Eur J Clin Invest* **35**, 711–717.
54 Pietrzak M, Shillito RD, Hohn T & Potrykus I (1986) Expression in plants of two bacterial antibiotic resistance genes after protoplast transformation with a new plant expression vector. *Nucleic Acids Res* **14**, 5857–5868.
55 Weigel D & Glazebrook J (2002) Transformation of *Agrobacterium* using the freeze–thaw method. *In Arabidopsis, A Laboratory manual*, Cold Spring Harbor Laboratory Press, New York, pp 125–126.
56 Clough SJ & Bent AF (1998) Floral dip‘ simplified method for *Agrobacterium*-mediated transformation of *Arabidopsis thaliana*. *Plant J* **16**, 735–743.
57 Peter E & Grimm B (2009) GUN4 is required for post-translational control of plant tetrapyrrole biosynthesis. *Mol Plant* **2**, 1198–1210.
58 Aebi H (1984) Catalase in vitro. *Methods Enzymol* **105**, 121–126.
59 Saleh L & Plieth C (2009) Fingerprinting antioxidative activities in plants. *Plant Methods* **5**, 2.
60 Rius SP, Casati P, Iglesias AA & Gomez-Casati DF (2006) Characterization of an *Arabidopsis thaliana* mutant lacking a cytosolic non-phosphorylating glyceraldehyde-3-phosphate dehydrogenase. *Plant Mol Biol* **61**, 945–957.
61 Taketani S & Tokunaga R (1982) Purification and substrate specificity of bovine liver-ferrochelatase. *Eur J Biochem* **127**, 443–447.
62 Kruft V, Eubel H, Jansch L, Werhahn W & Braun HP (2001) Proteomic approach to identify novel mitochondrial proteins in *Arabidopsis*. *Plant Physiol* **127**, 1694–1710.
63 Werhahn W, Niemeyer A, Jansch L, Kruft V, Schmitz UK & Braun H (2001) Purification and characterization of the preprotein translocase of the outer mitochondrial membrane from *Arabidopsis*. Identification of multiple forms of TOM20. *Plant Physiol* **125**, 943–954.
64 Laemmli UK (1970) Cleavage of structural proteins during the assembly of the head of bacteriophage T4. *Nature* **227**, 680–685.
65 Bollag DM, Rozycki MD & Edelstein SJ (1996) *Protein methods*, 2nd edn. Wiley-Liss, New York.
66 Bradford MM (1976) A rapid and sensitive method for the quantitation of microgram quantities of protein utilizing the principle of protein-dye binding. *Anal Biochem* **72**, 248–254.

Supporting information

The following supplementary material is available:
Fig. S1. AraCyc heme biosynthetic pathway.
Fig. S2. Determination of catalase activity in isolated mitochondria in the presence of protoporphyrin and Fe(II).
Table S1. Oligonucleotide primers used.

This supplementary material can be found in the online version of this article.

Please note: As a service to our authors and readers, this journal provides supporting information supplied by the authors. Such materials are peer-reviewed and may be re-organized for online delivery, but are not copy-edited or typeset. Technical support issues arising from supporting information (other than missing files) should be addressed to the authors.